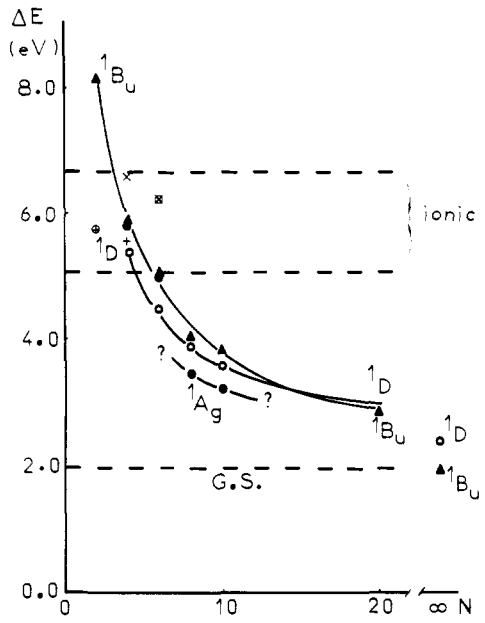

Figure 3. Energy from the planar ground state (ΔE) of the different vertical (^1A_g and ^1B_u) and twisted (ionic and diradicalar) excited states as a function of the number of carbons (N). (▲) ^1B_u vertical excited states, values for $n = 4, 6, 8$ from Table I,[9] and $n = 10, 20, \infty$ from Figure 1 of ref 3b. (●) ^1A_g vertical excited states, values for $n = 4, 6$ assuming near degeneracy with the ^1B_u state, for $n = 8$ from ref 6a, $n = 10$ from ref 34. (○) Twisted diradicalar excited states calculated adding a 2 eV ground state rotational barrier to the excitation energies reported in Table II. $n = \infty$ value extrapolated from the $n = 4$–10 ones by using a $A + B/n$ least-squares fitting with $r^2 = 0.997$. (⊕) M^+M^- ionic state for twisted and pyramidalized ethylene; (×) M^+A^- ionic state for twisted and C_2-pyramidalized butadiene; (+) M^-A^+ ionic state for twisted and C_1-pyramidalized butadiene; (⊗) A^+A^- ionic state for central bond twisted and C_3-pyramidalized hexatriene.

has not been established. Figure 3 shows the value reported for octatetraene[6a] and 2,10-dimethylundecapentaene.[34] In this figure the energies of the terminally twisted neutral excited states have been estimated by adding the lowest transition energy of a ($2n - 1$) polyene (Table II) to a 2 eV ground state rotational barrier. Figure 3 also exhibits the approximate position of the ionic funnels, which, according to Section III, should lie at an almost constant level between 5.1 and 6.7 eV.

(34) R. L. Christensen and B. E. Kohler, *J. Chem. Phys.*, **63**, 1837 (1975).

VI. Conclusion Concerning the Linear Polyenes

The qualitative conclusions of the preceding discussion result directly from Figure 3.

The photoisomerization of isolated ethylenic bonds is likely to proceed through the ionic funnel, which is much below the vertical $\pi\pi^*$ excited state. For butadiene our extended basis set calculation exhibits a twisted pyramidalized ionic level at 129 kcal/mol (i.e., 5.62 eV) above the planar ground state. The quantitative description of these ionic states requires the use of diffuse AO's and 3d AO's (the best calculations of the vertical transition to the ^1B_u state of butadiene exagerate this transition by 1 eV[4b,25]) and our value must be considered as an upper bound; the vertical excitation brings 6 eV to the molecule, and the photoisomerization of this molecule may proceed through the ionic funnel, although a neutral funnel is close in energy.

For hexatriene the 6.21 eV vertical ^1B_u absorbing state and the ionic twisted minimum should be close in energy, while a neutral twisted funnel should be somewhat below: our minimal basis set calculations (5.1 eV) without appropriate geometry optimization should represent an upper bound for this funnel concerning the torsion around the central bond, and our schematic model reported in Figure 3 suggests a 4.5 eV funnel for the torsion around the terminal bond. For this molecule the diradicalar funnel begins to appear as the main candidate for the isomerization process.

For larger polyenes the rapid decrease of the (G–S → ^1B_u) vertical transition energy makes impossible the travel through the ionic twisted minima while the twisted diradicalar funnels are low enough to be reached. One is always in case c of Figure 2 and the photoisomerization requires a decay to the lowest neutral diradicalar excited state (one may also conceive nonradiative decay to the vibrational levels of the ground state).

Acknowledgment. I.N. thanks the Ministerio de Universidades e Investigacion of Spain for a postdoctoral fellowship.

Registry No. Ethylene, 74-85-1; butadiene, 106-99-0; hexatriene, 2235-12-3; styrene, 100-42-5.

Semiconductor Interface Characterization in Photoelectrochemical Solar Cells: The p-InP (111)A Face

H. J. Lewerenz,[‡] D. E. Aspnes, B. Miller, D. L. Malm, and A. Heller*

Contribution from Bell Laboratories, Murray Hill, New Jersey 07974.
Received September 23, 1981

Abstract: Spectroscopic ellipsometry and low-energy (helium) ion scattering spectroscopy show the formation of hydrated indium oxide on the (111)A (indium) face of p-InP when the crystal is etched in either air-saturated acid or methanol–bromine, or when used as photocathode in the p-semiconductor liquid junction solar cell. The stability and efficiency of the cell depend on the presence of a thin, large band gap layer of indium oxide. The relatively better performance of p-InP over p-GaAs in such a cell is attributed to the different oxide surface chemistry of the latter, which leads to contamination by elemental arsenic. The favorable performance of p-InP in the V(II)–V(III)–HCl cell is ascribed to the reduction of recombination sites in the forbidden gap by termination of the lattice by the oxide.

1. Introduction

Various strategies have been employed to overcome instabilities encountered in photoelectrochemical regenerative solar cells. Cells based on p-type semiconductors[1] have the intrinsic advantage of cathodic protection of the illuminated semiconductors.[2,3] We have

[‡]Hahn-Meitner-Institut für Kernforschung Berlin GmbH, D-1000 Berlin 39, West Germany.

(1) R. Memming in "Semiconductor Liquid Junction Solar Cells", A. Heller, Ed., The Electrochemical Society, Princeton, N. J., 1977, p 38.

0002-7863/82/1504-3325$01.25/0

reported the development of an efficient and stable solar cell using p-InP as the photocathode with a solar-to-electrical conversion efficiency of 9.4% under solar illumination close to AM1 conditions, recently increased to 11.5%.[2] We have also reported on p-InP photocathodes with noble metals incorporated in the surface which reduce the external electrical energy required for hydrogen evolution from aqueous electrolytes. The energy saved amounts to 12% of the incident sunlight.[4-6]

The present investigation focuses on the interfacial properties of p-InP photocathodes in aqueous acids that give rise to their desirable characteristics.[2,4-9] Surface-sensitive techniques have been employed and the results analyzed for their implications to the construction of efficient and stable liquid-junction solar cells.

2. Experimental Section

InP, grown by the gradient freeze technique and doped p-type with 2.4×10^{17} cm^{-3} Zn, was cut from a single-crystal boule to yield (111) faces. The carrier mobility was 87 cm^2 V^{-1} s^{-1} and the bulk resistivity was 0.287 Ω cm. A faces of the (111) planes were prepared by polishing with an alumina slurry followed by etch-polishing on lens paper impregnated with methanol–x% bromine solution, with x varying from 2% in the initial to 0.05% in the final stage of polishing.

A low-reflectance matte black surface was obtained by repeatedly dipping the crystal for 10 s in 2:2:1 H_2O:HNO_3:HCl and rinsing for 20 s with deionized water. The total exposure time of the sample to the etchant was 2 min. The back contact was made by first evaporating 300-Å Zn, then 1000-Å Au, and heating to 450 °C. The treatment forms a p^+ region which is contacted by the Au–Zn.

The (100) p-GaAs single crystals were Cd doped to 2×10^{16} cm^{-3}. Ohmic back contacts were made as for p-InP. Electrodes were epoxy mounted. Solutions were prepared from "electronic grade" chemicals and deionized water. The solution containing the V(II)/V(III) redox couple was prepared by reacting 3 N purity V_2O_5 with 6 N Zn metal in water with addition of concentrated HCl sufficient to yield 4 M HCl after reaction. The solution potential typically used in the cell, −0.47 V vs. the saturated calomel electrode (SCE), could be adjusted to more negative values by adding Zn, or more positive ones by bubbling O_2. All electrochemical measurements were performed potentiostatically with spectral purity carbon rods as reference and as counterelectrodes. The solutions were magnetically stirred.

Spectroscopic ellipsometry, scanning electron microscopy (SEM), X-ray fluorescence, and low-energy ion scattering spectroscopy (LEISS) were used to characterize the semiconductor surfaces after air or electrolyte exposure. Since these techniques are well established, only necessary details are given in the appropriate sections.

3. Optical Determination of Interface Characteristics

The exceptional solar energy conversion efficiency of the p-InP/VCl_3–VCl_2–HCl/C cell,[2] and of cells based on indium oxide and indium junctions of other III–V compounds,[10] indicates a unique surface chemistry of p-InP. Spicer et al. found that chemisorption of submonolayer amounts of oxygen drastically shifts the surface Fermi level position.[11] Casey and Buehler have shown reduction in surface recombination velocity in air-exposed InP.[12] To obtain further information about the surface region, we have used spectroscopic ellipsometry which is highly surface sensitive and can be used to study in situ solid surfaces in equilibrium with liquid or gas ambients. The specific rotating-analyzer configuration used in these measurements has a spectral range 1.5–6.0 eV.[13]

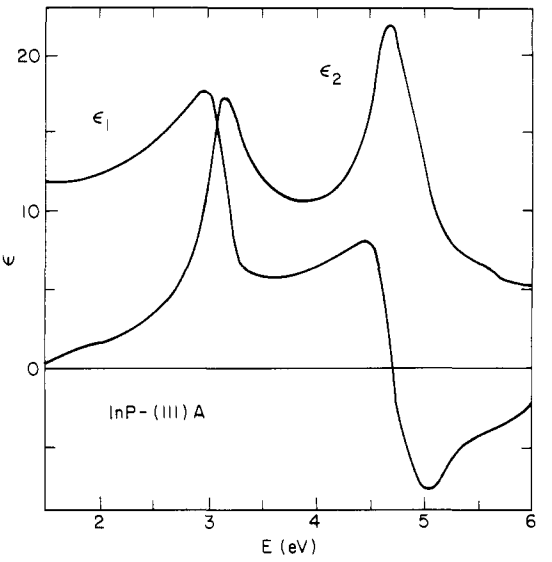

Figure 1. Spectral dependence of ϵ_1 and ϵ_2 for a high-quality InP (111)A face.

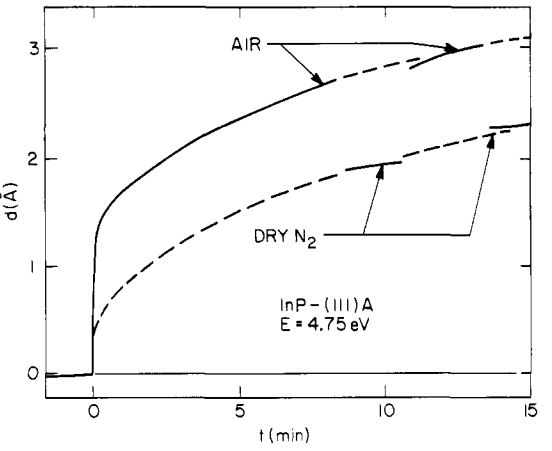

Figure 2. Influence of air exposure of ϵ_2 at its maximum value (4.78 eV) for InP (111)A. Solid lines are data; dashed lines are extrapolations taking into account the adsorbed volatile layer present in air but absent in dry N_2.

Because all layers to which light penetrates contribute to the overall dielectric response of a sample, it is necessary to determine the intrinsic dielectric response of InP before analyzing data on oxide overlayers. As discussed elsewhere,[14] it is generally not possible to obtain the true intrinsic response of any material by reflection techniques owing to the unavoidable presence of residual overlayers, but it is possible to obtain a best approximation by maximizing the value of ϵ_2 (the imaginary part of the complex pseudodielectric function $\epsilon = \epsilon_1 + i\epsilon_2$) at the energy corresponding to its absolute maximum, 4.87 eV for InP. The chemical treatment that achieves the sharpest discontinuity between substrate and ambient (equivalent to the highest quality surface with least amount of overlayer or microscopic roughness) yields the highest observed value of ϵ_2. We use the term pseudodielectric function because it is an average quantity calculated from the ellipsometrically measured complex reflectance ratio.[14]

We achieved the highest ϵ_2 value for this surface with a solution of methanol–0.05% bromine followed by a water rinse. Our most accurate representation of the true bulk dielectric function spectrum of InP is shown in Figure 1. Our observed peak value of $\epsilon_2 = 22.5$ should be compared with the previous best from Phillip

(2) (a) A. Heller, B. Miller, H. J. Lewerenz, and K. J. Bachmann, *J. Am. Chem. Soc.*, **102**, 6555 (1980); (b) A. Heller, B. Miller, and F. A. Thiel, *Appl. Phys. Lett.*, **38**, 282 (1981).
(3) F. R. F. Fan and A. J. Bard, *J. Am. Chem. Soc.*, **102**, 3677 (1980).
(4) A. Heller and R. G. Vadimsky, *Phys. Rev. Lett.*, **46**, 1153 (1981).
(5) A. Heller, *Acc. Chem. Res.*, **14**, 154 (1981).
(6) A. Heller, W. D. Johnston, Jr., H. J. Leamy, B. Miller, and K. E. Strege, Proceedings of the 15th IEEE Photovoltaic Specialists Conference, Orlando, Fla., May 12–15, 1981.
(7) S. Menezes, H. J. Lewerenz, F. A. Thiel, and K. J. Bachmann, *Appl. Phys. Lett.*, **38**, 710 (1981).
(8) M. P. Dare-Edwards, A. Hamnett, and J. B. Goodenough, *J. Electroanal. Chem.*, **119**, 109 (1981).
(9) R. N. Dominey, N. S. Lewis, and M. S. Wrighton, *J. Am. Chem. Soc.*, **103**, 1261 (1981).
(10) K. J. Bachmann, H. Schreiber, W. R. Sinclair, P. H. Schmidt, F. A. Thiel, E. G. Spencer, G. Pasteur, W. L. Feldman, and K. J. StreeHarsha, *J. Appl. Phys.*, **50**, 3441 (1979).
(11) W. E. Spicer, I. Lindau, P. Skeath, C. Y. Su, and P. W. Chye, *Phys. Rev. Lett.*, **44**, 420 (1980).
(12) H. C. Casey and E. Buehler, *Appl. Phys. Lett.*, **30**, 247 (1977).
(13) D. E. Aspnes and A. A. Studna, *Appl. Opt.*, **14**, 220 (1975); *SPIE Proc.*, **112**, 62 (1977); *Rev. Sci. Instrum.*, **49**, 291 (1978).
(14) D. E. Aspnes, *J. Vac. Sci. Technol.*, **17**, 1057 (1980).

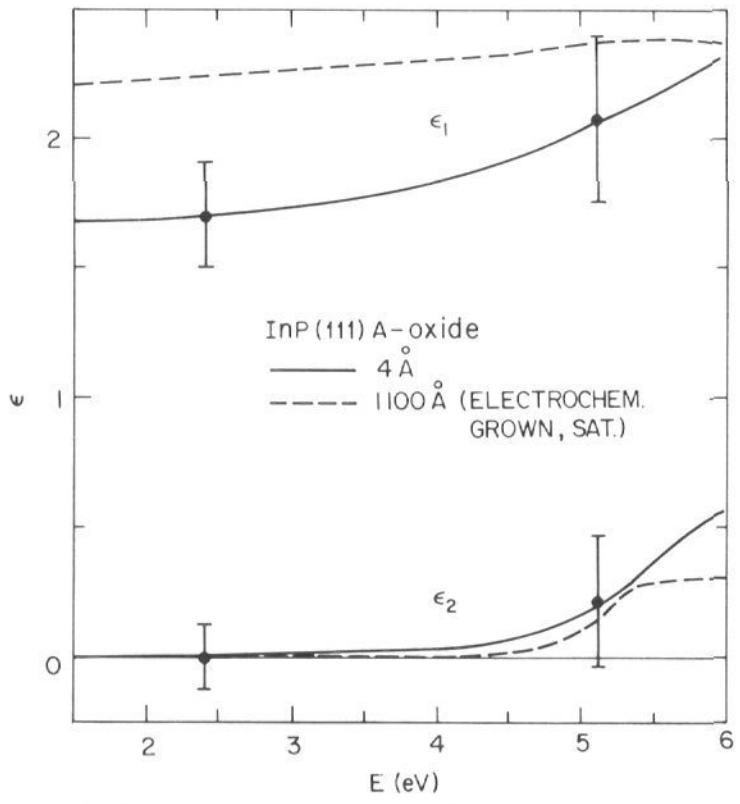

Figure 3. Optical properties of a surface film on InP (111) formed after exposure to laboratory air and successive flow of dry N_2 gas toward the sample. The spectral dependence of ϵ_1 and ϵ_2 for the saturated electrochemically grown anodic oxide on InP is shown for comparison (dashed lines).

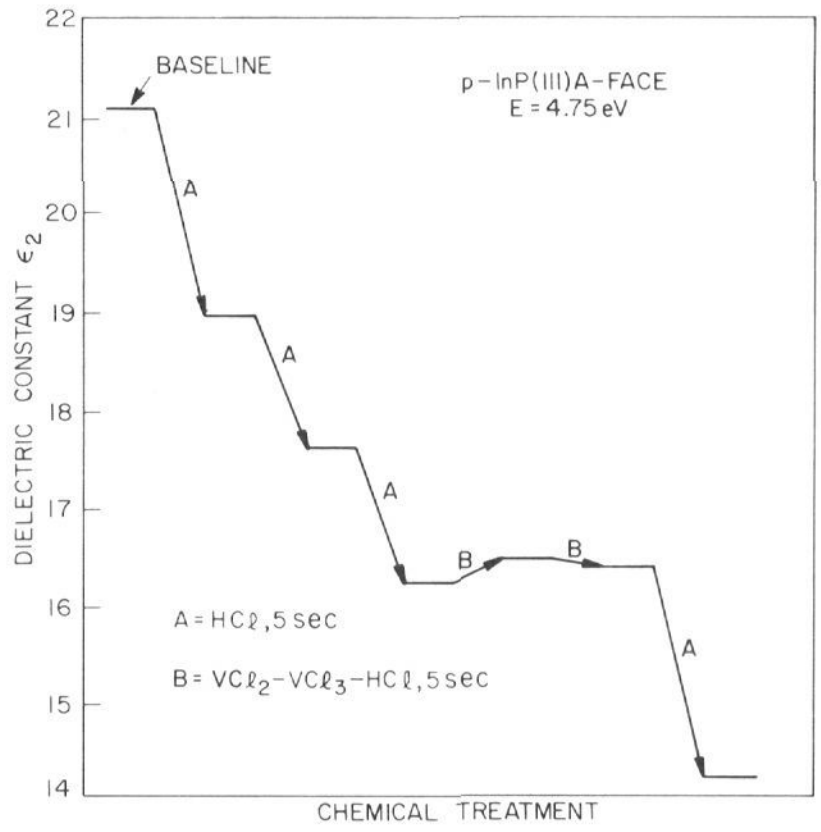

Figure 4. Influence of chemical treatment on ϵ_2 of InP (111) at its maximum value at 4.75 eV.

and Ehrenreich[15] who reported 19.7.

The formation of oxide and contaminant overlayers was inhibited during measurement by keeping the sample in flowing dry N_2. When the flow was shut off, exposing the sample to room air, a layer, characteristic of all samples, is rapidly formed as indicated in Figure 2. Here, pseudodielectric function data were measured as a function of time at a fixed energy, $E = 4.75$ eV. The sample was exposed to air at $t = 0$, leading to the rapid, reversible accumulation of an adsorbed overlayer of 1-Å average thickness and a gradual buildup of a nonvolatile overlayer, as indicated. The dashed curves are extrapolations corresponding to unmeasured portions of the curves with and without the volatile overlayer present. The thickness scale was determined from an exact solution of the three-phase model[16] using previously determined values of the substrate dielectric function and those determined for the overlayer (see below).

The dielectric response of the overlayer in slightly thicker form is shown in Figure 3 together with that measured for a thick electrochemically grown anodic oxide film that had been exposed to air until saturation conditions had been obtained.[17] The thickness was determined by requiring that ϵ_2 be zero in the region of transparency. Error bars refer to the approximate uncertainty as determined from scatter in the data. Basically, the properties of the thin overlayer are remarkably similar to those of the saturated oxide film except that ϵ_1 is reduced. This is probably due to greater porosity of the thin layer and is consistent with either 20% voids or 30% water as calculated by the effective medium theory.[18] The absorption edge at 4.5 eV corresponds closely to that of the saturated oxide, though it is somewhat higher than the 3.8-eV edge of nonhydrated In_2O_3.[19]

Although HCl is known to etch the A face of InP (111), the electrodes, when kept 1 week in the 4 M HCl redox couple solution, did not show corrosion in the dark or under illumination.[2] We examined the effects on ϵ_2 values (at 4.75 eV) of the (111) A faces caused by both concentrated oxygen-free HCl and the V(II)–V(III)–HCl–Zn solution. As shown in Figure 4 the in situ HCl treatment by itself causes a pronounced decrease of ϵ_2, attributed to surface roughening. The vanadium solution did not further alter ϵ_2, but a subsequent exposure to HCl caused an additional decrease in ϵ_2. These results indicate a successive surface roughening of InP upon repeated HCl–H_2O cycles and a lack of substantial etching in the V(II)–V(III) solution or other oxygen-free solutions. When p-InP (111)A and -B samples were kept in two 1:1 HCl:H_2O solutions, respectively saturated with nitrogen or air, after 120 h, no measurable weight loss was found for the sample in nitrogen/HCl, whereas the sample in air/HCl dissolved at a rate of about 10 mg/cm^2·h. Nevertheless, even the "stable" sample developed a matte black finish on the A face and was shiny gray on the B face, showing at least some attack. This etch level may, however, be due to oxidation by a trace impurity (such as $FeCl_3$) in HCl. Clearly, direct attack by hydrogen ions must be very slow, and the surface roughening by HCl/H_2O cycles involves oxidation by dissolved oxygen.

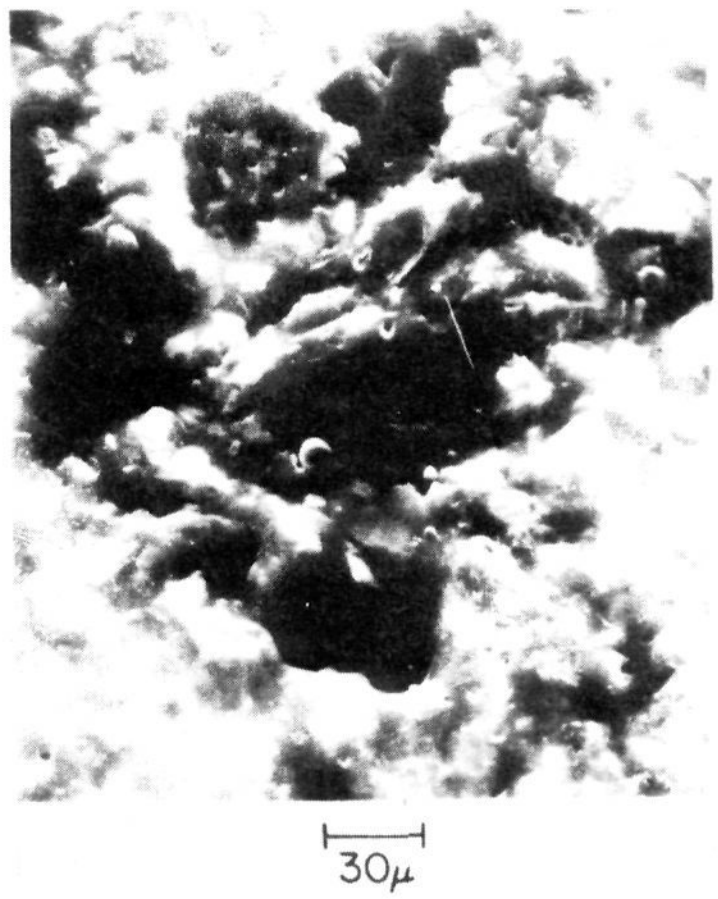

Figure 5. Electron micrograph of matte black etched A face of InP (111).

The weight-loss data in a nitrogen-scrubbed solution, which corresponds to the condition in the presence of a strong reducing

(15) H. R. Phillip and H. Ehrenreich, *Phys. Rev.*, **129**, 1550 (1963).
(16) D. E. Aspnes, in "Optical Properties of Solids: New Developments", B. O. Seraphin, Ed., North-Holland, Amsterdam, 1976, p 799.
(17) A. A. Studna and G. J. Gualtieri, *Appl. Phys. Lett.*, **39**, 965 (1981).
(18) D. A. G. Bruggeman, *Ann. Phys. (Leipzig)*, **24**, 636 (1935).
(19) Y. Ohhata, F. Shinoki, and S. Yoshida, *Thin Solid Films*, **59**, 255 (1979).

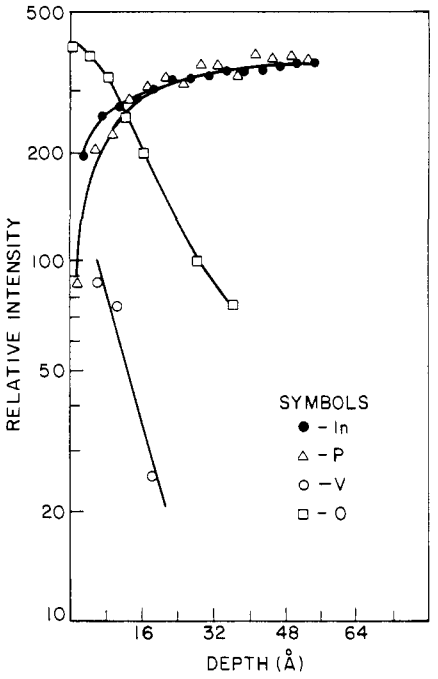

Figure 6. LEISS depth profile of p-InP after V(II)/V(III)/HCl cell cycling to reproducible characteristic.

agent (V^{2+}), show that the attack on both the p-InP surface and its thin oxide must be insignificant. Otherwise the cyclic oxide formation–dissolution process would enhance the attack of the substrate. Very long term studies would be required to define the level of attack, as it is so low.

4. Structure and Composition of the Photoactive Surface

An electron micrograph of a surface exhibiting the matte black finish applied in solar cell runs[2] is shown in Figure 5. It is found that the introduced roughness is due to micron-size features. The "glassy" appearance of the matte black surface suggests that large areas consist of relatively smooth parts. It also appears that preferential etching by the 2:2:1 H_2O:HNO_3:HCl etch results in a lamellar-like surface structure.

Analysis of the surface region of a matte black etched sample by X-ray fluorescence, with only water used for rinsing, revealed traces of Zn and V. Prerinsing the sample with 0.01 M HCl removed the Zn and lowered the V surface concentration considerably, suggesting that vanadium oxides, hydroxides, or oxychlorides are merely precipitated on the surface by hydrolysis of vanadium chlorides upon rinsing by water.

The A face of a p-InP (111) single-crystal specimen was examined by LEISS (low-energy ion scattering spectroscopy) after the following sequence. The surface was first polished with an Al_2O_3 slurry, then etched in 2% bromine–methanol, and thoroughly rinsed in distilled water. The slice was then operated as an electrode in the V(II)/V(III)/HCl electrolyte, as described below under voltammetric behavior. Subsequent to cycling, the sample was removed from the cell, rinsed with acidified water and distilled water, and dried.

For LEISS a 1.5-keV He probe-ion beam was focused to a 1-mm spot for both sputtering and analysis. The backscattered ion energy range of interest was scanned at 2-min intervals. The sputter rate was estimated as 2 Å/min after calibration against a silver film of known thickness (quartz oscillator thickness monitor) vacuum deposited on InP.

A typical depth profile of the respective backscattered peak intensities is shown in Figure 6. The major elements, In and P, were detected across the total depth (≈30 Å) sampled, while oxygen and a high In/P ratio were found only in the near-surface region. The initial (surface) levels of oxygen and the high indium/phosphorus ratio decline steadily, indicative of the presence of a <4-Å thick indium and oxygen-containing layer. The profile "tail" is due principally to a sample beam-edge effect. A uniform, pure InP composition is reached at a depth between 4 and 10 Å. Zn and other impurities were not detectable at the 1 atom % level in the surface region.

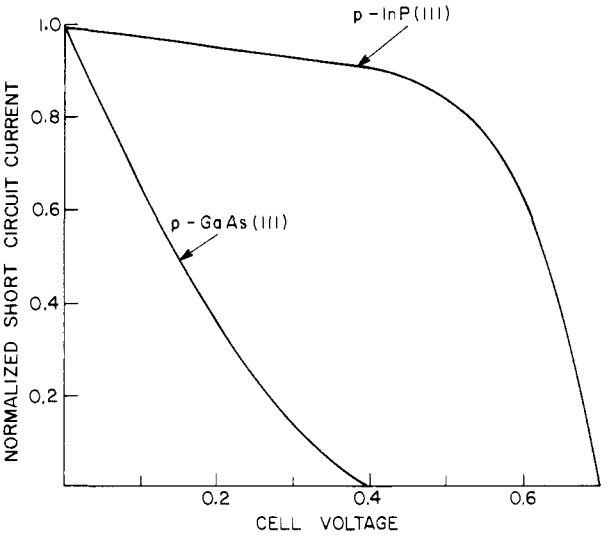

Figure 7. Comparison of output power characteristics of p-InP and p-GaAs photocathodes in V(II)/V(III) redox solution upon illumination by a 150-W tungsten iodine lamp; the short circuit current density has been normalized for better comparison.

No substantive layer of uniform oxygen content is found, and there is no evidence for the formation of an oxide of well-defined stoichiometry. This lack of stoichiometry is consistent with the observed changes in the In/P ratio in the region in which oxygen is detected. The declining oxygen content and the simultaneous increase in the P/In ratio suggest a gradual change from indium oxide or hydrated indium oxide at the very surface to InP in the bulk, with a shallow 4–10-Å thick region in which both are present.

5. Voltammetric Behavior

The power output characteristics of cells with p-InP (111)A and p-GaAs (100) faces in V(II)/V(III) redox solution are compared in Figure 7 for normalized short-circuit current density. The characteristics for the p-InP (100) and p-InP (111)B faces do not differ substantially from those obtained with the p-InP (111)A face. The performance of p-InP is clearly superior. The p-GaAs cell shows a fill factor (FF) < 0.25 and an open circuit voltage (OCV) of 0.4 V, whereas p-InP has FF = 0.61 and OCV = 0.7 V.

6. Discussion

A. Chemistry of the InP (111)A Face. Termination of the InP lattice disrupts the tetrahedral bonding, leaving on the (111)A plane a surface of In atoms, bound to three neighboring P atoms in the plane below. The remaining bond is available for chemisorption of ambient constituents. The ellipsometric data in Figure 2 establish that, upon exposure to air and moisture, an overlayer forms on the A face of InP (111). As noted, this overlayer contains a component volatile in a dry nitrogen system. The remaining surface film exhibits optical properties similar to those of the air-exposed InP (111)A face, suggesting an indium oxide film of an average thickness of 4 Å.

Indium metal forms hydrated indium oxide in the presence of water and air. The behavior of the InP (111)A face, seen by ellipsometry, suggests a surface consisting of indium oxide and water with the latter removed by dry nitrogen. When the InP (111) electrodes are exposed to the V(II)/V(III) redox couple solution, an oxide-type layer appears to form (Figure 6).

B. Electronic Properties of the Interface. The hypothetically clean InP (111)A face would tend to react with chemical species from the ambient. The ellipsometric data (Figures 2a and 3) give evidence of film formation at the semiconductor/air interface. Importantly for the photoelectrochemical cell, a 4–10-Å oxide on InP (111), related to that identified by ellipsometry for wet-air exposure, is maintained even in the presence of a strong acid. This

layer allows charge transfer across the interface via electron tunneling. The cell thus has formally a semiconductor–oxide–redox couple system, resembling metal–insulator–semiconductor or metal–oxide–semiconductor cells, though the oxide thickness is much less than common in these.

Surface oxidation displaces surface states in the band gap so as to increase the energy gap between neighboring states, thus reducing the cross sections for nonradiative electron-hole recombination.[5] These cross sections, like other radiationless relaxation processes, depend on the energy gap between the initial and final states. The larger the gaps the smaller the cross sections, because removal of large amounts of energy by collision with phonons is unlikely. Recently, we reported that the performance of the p-InP/VCl_3–VCl_2–HCl/C cell was improved also by the chemisorption of submonolayer amounts of silver at specific sites on the p-InP surface.[6] The effects of both oxygen and silver on the surface of p-InP resemble the effect of chemisorption of a submonolayer of Ru^{3+} and Pb^{2+} on n-GaAs surfaces and grain boundaries. Strengthening of the bonds at n-GaAs surfaces by reaction with Ru^{3+} has been shown to reduce the recombination velocity.[5,20]

We also note that an oxide of submonolayer thickness was shown by Spicer et al.[11] to substantially shift the surface Fermi level from the proximity of the valence band maximum to that of the conduction band minimum and to change the spacings of the acceptor and donor surface states. In this light, the performance of the new cell appears to result from the conjunction of two favorable effects: (a) enhanced protection against photocorrosion of the surface, which in principle holds for all p-type semiconductors in photoelectrochemical solar cells; (b) chemical changes resulting in a redistribution of states of the (111) surface, reducing recombination, and thus favorable to efficient charge transfer. We interpret these latter modifications as resulting from the existence of a thin, surface oxide film. In the case of GaAs, the arsenic oxide containing phase reacts with GaAs to form elemental arsenic, a semimetal, at the GaAs/oxide interface.[21-26] The resulting surface contains electronic states associated with As at the surface, which reduce the energy gaps crossed in the steps of the radiationless recombination process and lead to a high surface recombination cross section that lowers the fill factor and the open circuit voltage.

7. Conclusions

Spectroscopic ellipsometry and low-energy ions scattering spectroscopy show that the (111)A (indium) face of p-InP consists of hydrated indium oxide. The thickness of this layer is 4 Å. Below this layer one finds, to a maximum depth of 10 Å, a mixture of two phases, hydrated indium oxide and indium phosphide. At depths exceeding 10 Å, one finds only pure InP. We attribute the low electron-hole recombination velocity at the p-InP–HCl interface to termination of the lattice without the generation of weak or "dangling" bonds that could give rise to states with high recombination cross sections.

Acknowledgment. We thank K. J. Bachmann, W. A. Bonner, and F. A. Thiel for p-InP crystals, R. G. Vadimsky for electron micrographs, and S. M. Vincent for X-ray fluorescence measurements.

Registry No. InP, 22398-80-7.

(20) R. J. Nelson, J. S. Williams, H. J. Leamy, B. Miller, H. J. Casey, Jr., B. A. Parkinson, and A. Heller, *Appl. Phys. Lett.*, **36**, 76 (1980).

(21) Thurmond, C. D., Schwartz, G. P., Kamlott, G. W., and Schwartz, B., *J. Electrochem. Soc.*, **127**, 1366 (1980).

(22) Schwartz, G. P., Griffiths, J. E., DiStefano, D., Gualteri, G. J., and Schwartz, B., *Appl. Phys. Lett.*, **34**, 742 (1979).

(23) Watanabe, K., Hashiba, M., Hirohaata, Y., Nishino, M., and Yamashina, T., *Thin Solid Films*, **56**, 63 (1979).

(24) Schwartz, G. P., Griffiths, J. E., and Schwartz, B., *J. Vac. Sci. Technol.*, **16**, 1383 (1979).

(25) K. W. Frese and S. R. Morrison, *J. Electrochem. Soc.*, **126**, 1235 (1979).

(26) K. W. Frese, M. J. Madou, and S. R. Morrison, *J. Electrochem. Soc.*, **128**, 1939 (1981).

Vibrational Circular Dichroism in Amino Acids and Peptides. 4. Vibrational Analysis, Assignments, and Solution-Phase Raman Spectra of Deuterated Isotopomers of Alanine

Max Diem,*[1a] Prasad L. Polavarapu,[1b] Mohammedreza Oboodi,[1b] and Laurence A. Nafie*[1b,c]

Contribution from the Departments of Chemistry, City University of New York, Hunter College, New York, New York 10021, and Syracuse University, Syracuse, New York 13210.
Received August 14, 1981

Abstract: The complete vibrational frequency assignments for alanine-d_0, alanine-C^*-d_1, alanine-C-d_3, alanine-C-d_4, and alanine-N-d_3 in aqueous solution are presented. The assignments are based primarily on solution-phase Raman spectra, with results of infrared and Raman solid-phase spectra, a Urey–Bradley normal coordinate analysis, and existing literature data also taken into consideration. The new spectra have led us to a self-consistent assignment, and, with the exception of a few modes where skeletal stretching and rocking motions are strongly mixed, the observed spectra may be interpreted well in terms of group frequencies and predominantly local motions. In this respect our results differ from previous investigations which postulate extensive vibrational coupling between all parts of the molecule. Results of this frequency assignment and vibrational analysis form the basis for the interpretation and calculation of the infrared vibrational circular dichroism spectra presented in the following papers.

Vibrational circular dichroism (VCD) spectra of amino acids and oligopeptides in aqueous solutions are of interest from both a theoretical and biophysical standpoint. VCD, and its companion technique, Raman optical activity, have recently begun to reveal sensitive structural and stereochemical details of molecules in solution,[2-5] and small peptides provide a closely related series of

(1) (a) City University of New York, Hunter College. (b) Syracuse University. (c) Alfred P. Sloan Foundation Fellow.

(2) Nafie, L. A.; Diem, M. *Acc. Chem. Res.* **1979**, *12*, 296.

0002-7863/82/1504-3329$01.25/0